Microstructural Characterization of Mechanically Activated ZnO-Cr$_2$O$_3$ System

Z.V. Marinković[1,], L.Mančić[2], P. Vulić[3], O.Milošević[2]*

[1]Center for Multidisciplinary Studies, University of Belgrade,

Kneza Višeslava 1a, Belgrade, Serbia-Montenegro

[2]Institute of Technical Sciences of Serbian Academy of Sciences and Arts,

Knez-Mihailova 35/IV, Belgrade, Serbia-Montenegro

[3]Faculty of Mining and Geology, Department of Crystallography,

Đušina 7, Belgrade, Serbia-Montenegro

Abstract

An equimolar mixtures of starting ZnO and Cr$_2$O$_3$ powders were mechanically activated by grinding using a planetary ball mill for various periods of time (40 to 320 minutes). Formation of nanocrystalline ZnCr$_2$O$_4$ as normal spinel structure at room temperature is detected in all samples - after ball-milling.

A detailed XRD structural analysis (lattice parameters, site occupancy, the average primary crystallite sizes, crystal lattice microstrains) is realized by the pattern decomposition technique, performed in accordance with the procedure based on Rietveld software KOALARIET-XFIT. Due to the importance of cation distribution on the chemical and physical properties of spinels, a study of site occupation factors of ZnCr$_2$O$_4$ spinels has been undertaken. Evaluated spinel non-stoichiometry is a result of the ZnO dissolving in the stoichiometric ZnCr$_2$O$_4$. The manner of ZnO incorporation into the spinel lattice is performed according to the procedure based on calculation of both formation and attachment energies. The calculation based on the atomistic methods for the simulation and description of the

perfect and defect spinel $ZnCr_2O_4$ crystal lattice has been made togheter with the determination of the individual structural defects.

Introduction

Oxide with the spinel structure are some of the most studied compounds in solid state sciences due to their wide range of applications as a humidity sensors [1], semiconductors [2], magnetic materials [3], catalysts [4], among others.

The general formula of oxide spinels is AB_2O_4, and the distribution configuration is represented as $^{IV}(A_{1-x}B_x)^{VI}(B_{2-x}A_x)O_4$. Normal spinels have $x=0$, whereas *inverse* spinels have $x=1$; any distribution is possible between the extremes. The unit cell contains 8 unit formulas and the symmetry is cubic, space group $Fd\overline{3}m$, with a cell edge close to 8Å [5-7]. The anionic array is described by the monovariant equivalent position *32e^u*, point symmetry $\overline{3}m$. The actual value of the free parameter *u*, (commonly known as the oxygen positional parameter) shows a slight deviation from 1/4 if the unit cell origin is taken at a centre of symmetry $\overline{3}m$, equiposition 16c. This deviation usually increase the volume ratio between the occupied A and B sites, respectively, *8a* (1/8, 1/8, 1/8), $\overline{4}3m$, and *16d* (1/2, 1/2, 1/2), $\overline{3}m$ [5-7].

Determination of the cation distribution is of considerable relevance because the theoretical interpretation of the chemical and physical properties of these compounds depends on this distribution [2-4,8]. Some of these materials are interesting also because they may become non-stochiometric, thus giving defective spinels.

Mechanochemistry is one of the most promising low temperature methods of synthesis. Nucleation process is initiated at room temperature, exhibiting more homogeneous

distribution, larger specific surface area and smaller particle size of products as compared with those, prepared by conventional solid state method [3,8].

To our knowledge, the phase transformation kinetics of ball-milled chromates has not yet been studied in detail by X-ray powder structure refinement method. Subject of this work is a detailed investigation of the structural features of $ZnCr_2O_4$ spinel phase synthesized from mixtures of starting ZnO and Cr_2O_3 powders by mechanochemical reactions in a planetary ball mill.

Experimental procedure

Mixtures of starting ZnO (Merck, p.a. 99%) and Cr_2O_3 (Fluka, p.a. 99%) powders in equimolar quantities were used in experimental procedures. Mechanical activation was performed by grinding (dry) of conventional prepared mixture of powders, in a continual regime in a planetary ball mill (Fritsch Pulverisette 5) in air during 0, 40, 80, 160 and 320 min. In a planetary ball mill a rotating disk carries vials that rotate in opposite direction. The rotation speed of the disk was 325 rpm and that of the vials was about 475 rpm. Zirconium oxide grinding balls (approx.10 mm in diameter) and bowls (volume 500 cm^3) were used with a ball to powder mixture mass ratio of 40:1.

The X-ray powder diffraction (XRPD) data of the unmilled and ball-milled samples were recorded using a Philips PW 1710 automated diffractometer with CuK_α radiation and graphite monochromator. Scans were taken with a 2θ step size of 0.02^0 and counting time of 5s. XRD patterns were collected in the range of 27-45^0 (2θ), since this is the range in which the strongest X-ray reflections of the initial (ZnO and Cr_2O_3) and synthesized ($ZnCr_2O_4$) phases present could occur. All peak positions were used in the determination of precise microstrucural parameters. Structural refinements were carried out using the Rietveld program Koalariet-Xfit [9]. The lattice parameters were deduced from XRD line positions using a

least-squares refinement method. Peak profiles were fitted with a pseudo-Voight function and asymmetry parameters were considered for peaks below 45^0 (2θ). The background was refined with a second degree polynomial function. Refinement continues till convergence is reached with the value of quality factor, GoF very close to 1 (varies between 1.11 and 1.25), which confirms the goodness of refinement.

Results and discussion

The XRD powder patterns recorded from unmilled and ball-milled mixtures are shown in Fig.1. The powder pattern of unmilled mixture contains only the individual reflections of ZnO (JCPDS cards 36-1451) and Cr_2O_3 (JCPDS cards 38-1479) phases. The intensity ratio of individual reflections is in accordance with the stoichiometric composition of the mixture 33% of ZnO and 67% of Cr_2O_3 by weight. It is evident from the Fig.1 that in the course of ball milling of mixtures, the $ZnCr_2O_4$ (JCPDS cards 22-1107) phase has been formed and its amount increased gradually with increasing milling time. After only 40 min milling, the formation of $ZnCr_2O_4$ has been noticed clearly due to the appearance of at least (220) ($2\theta=30.45^o$) and most strongest (311) ($2\theta=35.70^o$) reflections in the respective XRD pattern. It is also evident from the figure that the content of ZnO phase has been reduced to a large extent in comparison to Cr_2O_3 phase. It is indicates that the ZnO phase is much prone to deformation fault as all the reflections are sufficiently broadened, and suggested much more instability and reactivity of this oxide component. After 80 min milling, intensities of (220) and (311) reflections increased and another isolated (400) ($2\theta=43.30^o$) reflection of $ZnCr_2O_4$ phase appeared in the XRD pattern. At the same time the intensities of starting oxide reflections have been reduced further. Except the strongest (104) ($2\theta=33.64^o$) reflection, all other reflections of Cr_2O_3 are disappeared completely in the XRD pattern of 320 min milling sample.

All the XRD patterns are analysed employing Rietveld's powder structure and microstructure refinement analysis [9]. The crystal refinements were performed assuming space group $Fd\bar{3}m$. In the final refinements 18 parameters were fitted to the 910 data points: 1 scale factor, 2 background parameters, zero point for 2θ, 5 profile function parameters (2 for the Lorentzian/Gaussian mixing parameter and 3 for the width), the average crystallite size, the crystal lattice microstrain, the cell parameter a, volume of the unit cell V, weight percent of the phase wt, 2 parameters of the site occupancy, one for each equiposition $8a$ and $16d$, the oxygen positional parameter u and isotropic thermal parameters of the unit cell b.

It is evident from the Fig.1 that almost all the reflections of ball-miled samples are very much broadened as well as partially or completely overlapped. Therefore, microstructure characterization and phase content of different phases considering all the symmetry permitted reflections cannot be obtained with sufficient accuracy without adopting the Rietveld's software having both the microstructure and structure refinement facilities. For example, Fig.2 shows the quality of profile fitting in the 80 min milled sample.

Table 1 contains the results of quantitative XRD analysis, which is made as a part of structural refinement [9]. The content wt% of ZnO decreased very rapidly, whereas the wt% of Cr_2O_3 decreased rather slowly with increasing milling time. The formation of $ZnCr_2O_4$ phase is noticed in 40 min milled sample and the wt% of it increasing continuously from 24.9 to 77.8. In the course of milling when the particles of individual phases come in contact to each other at the time of ball-to-ball and/or ball-to vial wall collision, nucleation of nanocrystalline Zn-chromate particle then takes place by solid-state diffusion between them as both the particle size and collision temperature favours the formation mechanism.

The nature of variation of crystallite size and rms lattice strain of ZnO, Cr_2O_3 and $ZnCr_2O_4$ are shown in Fig.3 and Fig.4, respectively. Due to high-energy impact, crystallite sizes of both the ZnO and Cr_2O_3 phases come down to nanometric order with-in a very short

duration of milling and then decreased slowly with increasing milling time (Fig. 3). The rms microstrain, unlike the crystallite size variation, increased rapidly with milling time, signifies the influence of high-energy impact in producing enormous amount of lattice imperfections inside the ZnO lattice (Fig.4). The microstrain value of Cr_2O_3 changes a little in the examined milling time. Different behaviour could be explained by the great difference of the crystal lattice energy of ZnO and Cr_2O_3 being 4107.25 and 15186 kJ/mol, respectively.

The lattice parameter of mechanosynthesized $ZnCr_2O_4$ spinel phase is significantly high in comparison to JCPDS reported values (prepared by a heating mixture of ZnO and Cr_2O_3 at $900^{\circ}C$) and increased non-linearly and continuously with increasing time with different rates of increment (Tab. 2). This mismatch in lattice parameter indicates that the distribution of cations between tetrahedral and octahedral sites depends on the method of preparation of Zn-chromates. The variation in reported lattice parameter might result from the presence of non-stoichiomtery. Based on the very strong crystal field stabilization energy in octahedral coordination of low-spin Cr^{3+}, it was assumed that all the Cr^{3+} is present on the octahedral sites [4,5,7]. This is supported by the fact that all chromate spinels containing octahedral Cr^{3+} are normal [5,6]. Considering Zn^{2+} and Cr^{3+} cation radii a higher unit-cell parameter a, should therefore be associated with an increased Zn content.

The presence of the ZnO as an accompanying phase during the process of spinel synthesis is known [1,4,10]. Stoichiometric $ZnCr_2O_4$ has a face-centered cubic arrangement of oxygen ions, in which the Cr^{3+} ions occupy half of the octahedral and the Zn^{2+} ions fill one-eighth of the tetrahedral sites enclosed within the anion sublattice. With this distribution, the calculated lattice parameter of the crystal is 8.340Å. The variation in the experimental values in the range 8.321-8.359Å [4,7,10] may indicate the formation of a non-stoichiometric and defective material. It has been shown that atomistic simulation methods can be used to derive the formation energies of an ideal $ZnCr_2O_4$ crystal, as well as a set of isolated defects and also

defects cluster formation which form the basis of an interpretation of this lattice parameter variation [10]. According to this model, the different defect reactions associated with ZnO solution give rise to different combinations and concentrations of defects. Since each defect has a characteristic defect volume, the different reactions give rise to different changes in volume, which can be related to changes in the average lattice parameter. Two of them lead to a decrease in the lattice parameter, as zinc content increases, while others result in an increase of spinel unit cell [10]. It seems from these results that the most favourable manner in which excess of ZnO can be accomodated as isolated defects into the lattice is by distributing the divalent zinc ions over both octahedral and tetrahedral sites with charge compesation provided by either oxygen vacancies or zinc interstitials [10].

Conclusion

Nanostructured $ZnCr_2O_4$ powders have been prepared from equimolar mixture of ZnO and Cr_2O_3 powder by ball milling within a very short time period. The content of ZnO phase has been reduced to a large extent in comparison to Cr_2O_3 phase. This indicate that the ZnO phase is much prone to deformation fault and may suggested much more instability and reactivity of this oxide component

The lattice parameters of the cubic spinel depended on the preparation conditions. These changes are associated with the non-stoichiometry and defect structure. The unit cell is divided into octants and the origin is displaced. This deviation increases the volume ratio between the occupied tetrahedral and octahedral sites. Considering Zn^{2+} and Cr^{3+} cation radii in the spinel phase with higher unit-cell parameter a, should be richer in Zn. It was shown that increasing of milling time contributed to the dissolution of ZnO in the spinel in a higher degree. Also, the accumulation of stored energy during ball-milling through repeated

fragmentation and re-welding of small grains leads to creation of lattice distortion of $ZnCr_2O_4$ phase which is manifested in contraction /expansion of lattice parameter of this phase.

The experimental data presented in this study indicating that some zinc ions enter the chromium sub-lattice while others become intersticial, whilst oxygen vacancies are formed in place of zinc interstitials.

References

1. Pokhrel, S., Jeyaraj, B., Nagaraja, K.S., Humidity Sensing Properties of $ZnCr_2O_4$-ZnO Composites. *Mater. Lett.*, 2003, **4378**, 1-6.

2. Honeybourne, C.L. & Rasheed, R.K., Nitrogen Doixide and Volatile Sulfide Sensing Properties of Cooper, Zinc and Nickel Chromite. *J.Mater.Chem.*, 1996, **6**, 3, 277-283.

3. Bid, S. & Pradhan, S.K., Preparation of Zinc Ferrite by High-energy Ball-milling and Microstructure Characterization by Rietveld's Analysis. *Mat.Chem.Phys.*, 2003, **82**, 27-37.

4. Castiglioni, G.L., Minelli, G., Porta, P. & Vaccari, V., Synthesis and Properties of Spinel-type Co-Cu-Mg-Zn-Cr Mixed Oxides. *J. Solid State Chem.*,2000, **152**,526-532.

5. West, A.R., *Solid State Chemistry and its Applications*, John Wiley & Sons, New York (1984) pp. 569

6. O'Neill N. & Navrotsky A., Simple Spinels: Crystallographic Parameters, Cation Radii, Lattice Energies and Cation Distriburions. *Amer. Mineral.*, 1983, **68**, 181-194.

7. Sickafus, K.E., Wills J.M. & Grimes, N.W., Structure of Spinel. *J. Am. Ceram. Soc.*, 1999, **82**, 12, 3279-3292.

8. Manik, S.K., Bose, P.& Pradhan,S.K., Microstructure Characterization and Phase Transformation Kinetics of Ball-milled Prepared Nanocrystalline Zn_2TiO_4 by Rietveld Method. *Mat.Chem.Phys.*, 2003, **82**, 837-847.

9. Cheary, R.W. & Coelho, A.A., Programs XFIT and FOURYA, CCP14 Powder diffraction Library-Daresbury Laboratory, Warrington, England (1996)**.**

10. Grimes, R.W., Binks, D.J.& Lidiard, A.B., The Extent of Zinc Oxide Solution in Zinc Chromate Spinel. *Philosopical Magazine*, 1995, **72**, 3, 651-668.

Figure captions

Fig. 1 X-ray powder diffraction patterns of unmilled and ball-milled equimolar mixture $ZnO-Cr_2O_3$.

Fig. 2 X-ray diffraction patterns of the 80 min milled samples. The curves over the experimental points are the patterns calculated by Rietveld analysis [9]. The difference between the calculated and observed pattern is presented below the corresponding diffractogram.

Fig. 3 Variation of the crystallite size of ZnO, Cr_2O_3 and $ZnCr_2O_4$ with increasing milling time.

Fig. 4 Variation of the rms strain of ZnO, Cr_2O_3 and $ZnCr_2O_4$ with increasing milling time.

Table captions

Tab. 1 Quantitative XRPD analysis for unmilled and milled ZnO-Cr_2O_3 powder mixture.

Tab. 2 Crystallographic data of mechanosynthesized $ZnCr_2O_4$ spinel phase estimated from the Rietveld anlysis [9].
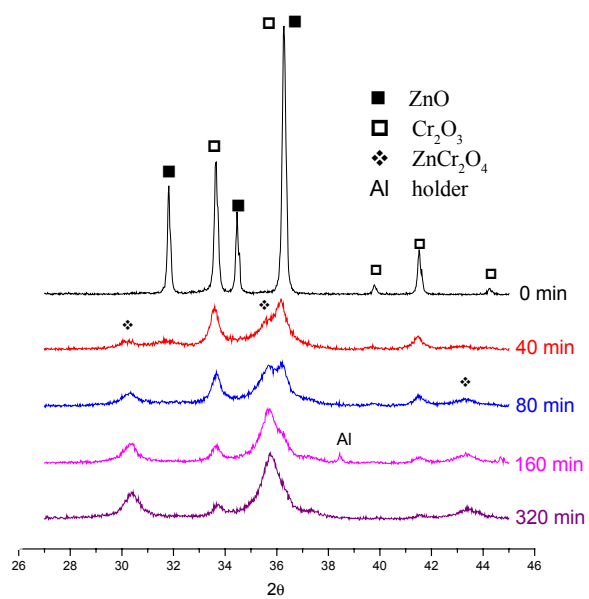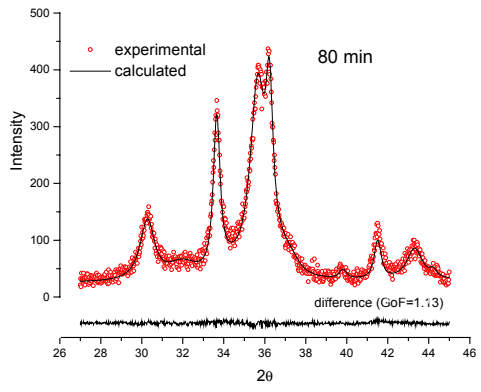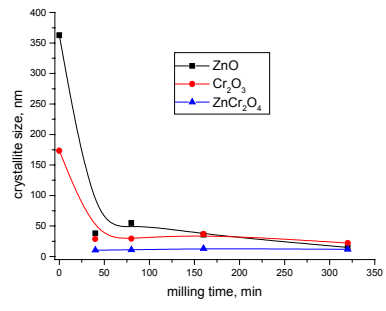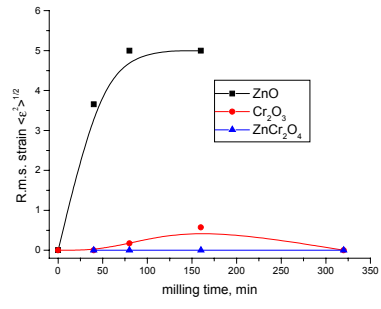
Fig.1

Fig.2

Fig.3

Fig.4

Table 1

	Weight percent, %		
Mill. time, min	ZnO	Cr_2O_3	$ZnCr_2O_4$
0	33	67	-
40	23.0	52.1	24.9
80	10.3	42.5	47.2
160	3.9	25.2	70.9
320	2.0	15.2	77.8

Table 2

Mill.time [min]	a [Å]	u	occup. $8a$	occup. $16d$
40	8.369	0.258	0.968	1.891
80	8.380	0.258	0.938	2.064
160	8.379	0.258	0.950	2.070
320	8.399	0.264	0.959	2.080